THE ROYAL SOCIETY

Quantum size effects in molecular magnets

By Dante Gatteschi

Department of Chemistry, University of Florence, via Maragliano 77, I-50144 Florence, Italy

The unique role of molecular clusters in the investigation of quantum size effects in magnetism is reviewed. The types of quantum effects to be expected in mesoscopic clusters, which can be obtained by a quasi-classical approach, are compared with those actually observed in molecular clusters. In particular, the focus of attention is put on antiferromagnetic rings, which show stepped hysteresis and anomalies in the proton relaxation behaviour. Ferrimagnetic clusters have been shown to undergo quantum tunnelling of magnetization, and have recently provided the first experimental evidence of the so-called Berry phase in magnets.

Keywords: molecular magnetism; nanomagnet; cluster; quantum tunnelling; quantum size effects; Berry phase

1. Introduction

Particles whose sizes are of the order of some nanometres in at least one direction are of great theoretical interest at the moment because they are the ideal systems for observing phenomena associated with the coexistence of quantum and classical effects (Jain 1989; Halperin *et al.* 1993). This point is well illustrated for conductors by so-called quantum layers, quantum wires and quantum dots, which correspond to nanometric in one, two and three directions, respectively. These materials are actively investigated for basic science, but they already provide many possibilities for application (Bastard & Brum 1986).

The same theoretical interest is also being developed for magnets, in which there is a strong expectation to be able to observe quantum effects in macroscopic particles (Caldeira & Leggett 1981; Gunther & Barbara 1995; Chudnovsky & Tejada 1998). The phenomena that are actively looked for are macroscopic quantum tunnelling of the magnetization, and macroscopic quantum coherence, where the magnetization, or the Néel vector, tunnel coherently between classically degenerate directions over many periods. These phenomena are interesting both from the fundamental point of view and from the perspective of possible applications, of which quantum computing is certainly one of the most exciting (Deutsch & Jozsa 1985). They can be collected under the label 'macroscopic quantum phenomena' (MQP).

Compared with the observation of quantum phenomena in conductors, the observation of macroscopic quantum effects in magnetic particles leads to some additional difficulties. In fact, tunnelling effects are easily destroyed, or masked, if the particles are not all identical, if they are not all iso-orientated and if the interactions between them are not suitably reduced to a minimum. Several attempts have been made to prepare nanosized magnetic particles that obey all these requisites, but so far no

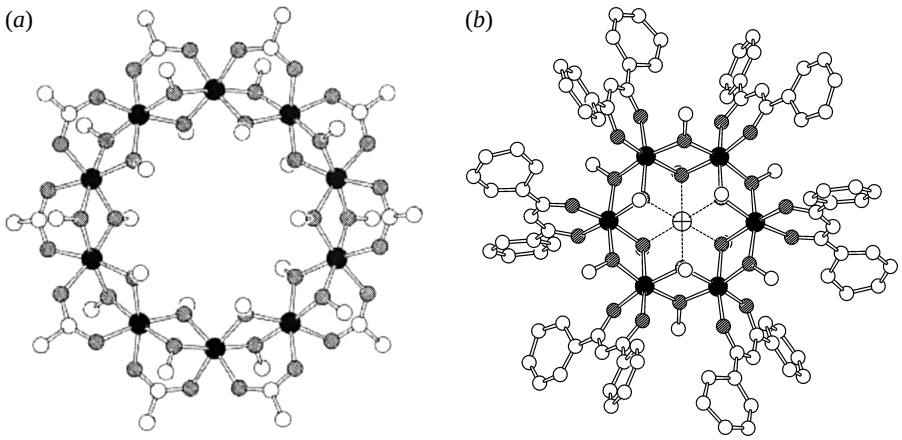

Figure 1. Structure of Fe10 and Fe6Li (after Taft & Lippard (1990) and Caneschi *et al*. (1996), respectively).

unambiguous success has been achieved. For instance, nanosized particles obtained by thermal decomposition of iron salts have been investigated by microSQUID techniques, but no clear evidence of quantum tunnelling was achieved. Analogous doubts were left by experiments performed both on the natural form of ferritin and on an artificially magnetite-loaded derivative (Awschalom *et al.* 1993; Gider *et al.* 1995, 1997; Garg 1995; Tejada 1995).

The situation was becoming static, when it was discovered that molecular magnetic clusters may provide unique possibilities for the direct measurement of all kinds of quantum size effects (Gatteschi *et al.* 1994). Two typical examples of molecular clusters are shown in figure 1. These are molecular objects, which can be synthesized with the techniques of molecular chemistry. They are all identical, their structures can be exactly known, in general through X-ray crystal structure determinations and in some cases also through neutron diffraction experiments. Furthermore, they can be dissolved in suitable solvents, in order to reduce to a minimum the magnetic interactions between them, or in polymer films, or even in Langmuir–Blodgett films. Finally, they can be produced in single crystals that contain a macroscopic number of identical magnetic subunits that are weakly coupled to each other as well as to their surroundings. Therefore, it is possible to investigate a macroscopic ensemble, and still measure the individual properties of the clusters.

These advantages prompted Stamp (1996) to write:

> Now the chemists have come to the rescue, working up from the atomic scale. The promise is of many new magnetic macromolecules, behaving like giant spins. That would truly prop open the door to the fledgling field of quantum nanomagnetism, perhaps leading to the nanomolecular engineering of magnetic memory elements that have inherently quantum properties.

However, there are also some obvious disadvantages, the largest of which is the fact that nobody has so far been able to prepare molecular clusters containing more than about 20 magnetic centres. Under these conditions, it is certainly difficult to call the clusters ‘macroscopic’ or even ‘mesoscopic’. However, this paper aims to show that

the quantum effects that can be observed in these rather complex objects already have the flavour of what is expected for MQP, or, better still, that they provide unique testing grounds for theories developed at the semi-classical level. In fact, molecular clusters provide evidence of the fact that MQP are a natural extrapolation of the properties observed in quantum sized objects. This is not a totally new observation. In fact, it was well known that the thermodynamic properties of one-dimensional materials may be rather accurately obtained by extrapolation of the properties of relatively small magnetic rings (De Jongh & Miedema 1974). Now, however, quantum effects observed in clusters shed light on the possible quantum phenomena to be observed in mesoscopic objects.

As is always the case in fields of multidisciplinary research, it is necessary first of all to adopt a common language in order to achieve the best results. Therefore, I will try first of all to clarify what is commonly understood for quantum tunnelling and quantum coherence in magnetic phenomena. Second, I want to report a few results obtained in the observation of MQP in molecular clusters, starting from rings and then passing to more complex structures.

2. Quantum tunnelling and quantum coherence

Macroscopic quantum tunnelling of the magnetization must be a rare event, because a macroscopic particle is, by definition, a system that is large enough to behave classically during most of the time it is being observed. There are several theories providing information on the frequency of the tunnelling, the most popular of which is that of the so-called instantons (Langer 1967). This theory is a general one that describes the tunnelling of the particle from the metastable state in which it is prepared, using imaginary time. For this reason, motion does not take any real time, occurring in imaginary time (Chudnovsky & Tejada 1998). The tunnelling rate is expressed in the form

$$\Gamma = A(T)\exp(-U_0/T_{\mathrm{esc}}(T)), \tag{2.1}$$

where U_0 is the height of the barrier and T_{esc} is the characteristic escape temperature. The pre-exponential factor is called the attempt frequency and it corresponds to the small oscillations near the bottom of the potential well. Typically, at high temperature $T_{\mathrm{esc}} = T$, i.e. the decay of the metastable state occurs through a thermal over-barrier transition. In the tunnelling regime, T_{esc} tends to a non-zero constant and the relaxation time becomes temperature independent.

The possibility of observing MQP is bound by the following conditions: (i) a barrier is present; and (ii) a suitable matrix element admixes states on the two sides of the barrier. Specializing to magnetic particles suggests a treatment that is an extension of the classical one for superparamagnetic particles. The magnetization of the particle can be either up or down, as shown in figure 2, and the barrier for reorientation is given by the axial magnetic anisotropy. The origin of the axial anisotropy is, in general, associated with magneto-crystalline anisotropy, i.e. with the contribution to the energy of the particle from the individual magnetic centres. For instance, rare earth ions, cobalt, manganese(III), are individual magnetic centres that tend to contribute a large magnetic anisotropy to the particles.

In the absence of suitable matrix elements connecting the two sides of the barrier, the magnetic particles can only reorient with a thermally activated mechanism. This

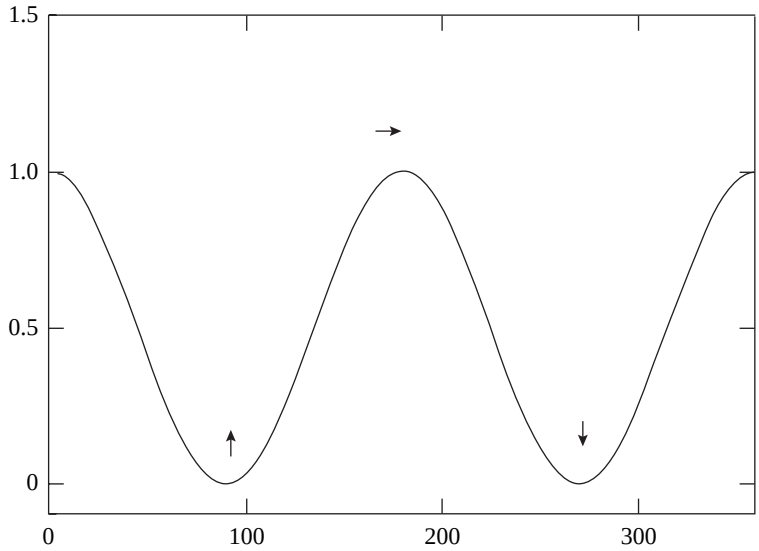

Figure 2. Two-well representation of the equilibrium states of the magnetization of a superparamagnetic particle.

gives rise to a relaxation time (Morrish 1966):

$$\tau = \tau_0 \exp(\Delta/kT). \tag{2.2}$$

However, if a suitable transverse field is present coupling the two states on the two sides of the barrier, the tunnelling mechanism becomes possible. The transverse fields can be provided by an external magnetic field, by magneto-crystalline contributions, by the dipolar fields within the particles, by the dipolar fields of the other particles that are unavoidably present in the investigated systems, or by the magnetic fields of the nuclei that are coupled to the electrons via the hyperfine interaction (Prokof'ev & Stamp 1996). It is important to recognize that in particles containing an odd number of unpaired electrons the only transverse field breaking Kramer's degeneracy is an external magnetic field. Therefore, it should not be possible to observe quantum tunnelling effects in Kramers species in the absence of an applied transverse field.

The existence of tunnelling is, therefore, associated with the removal of the degeneracy of a pair of magnetic levels by the action of a suitable transverse field. The two levels are separated by the energy

$$\Delta = h\Gamma/2\pi, \tag{2.3}$$

where Δ is the tunnel splitting. For macroscopic quantum tunnelling, the splitting Δ is always small compared with the attempt frequency. Therefore, the wave functions of the two low-lying states can be approximated by linear combinations of the degenerate states in the absence of tunnelling. If a single domain particle is in the true ground state, the probability of its magnetization having a certain orientation at a moment of time t oscillates with time:

$$\langle \boldsymbol{M}(t)\boldsymbol{M}(0)\rangle M_0^2 \cos(\Gamma t). \tag{2.4}$$

The system placed in a field of frequency Γ should show a resonance in the power absorption. This effect is called macroscopic quantum coherence (MQC). The observation of MQC is, however, hampered by the fact that interactions with the environment of order Δ may make its observation impossible. This is much more stringent than the condition for the observation of QTM, where dissipation towards other degrees of freedom of the system must be small compared with the attempt frequency, which is much larger than Δ.

Magnetic tunnelling has been investigated both in monodomain ferromagnetic particles, and in the Néel vector of antiferromagnetic particles. In particular, the phenomena that have been investigated are the quantum nucleation of magnetic domains, the quantum depinning of domain walls, and the relaxation of the magnetization. The investigated systems range from γ-Fe_2O_3 particles to $CoFe_2O_4$ particles to ferritin (Chudnovsky & Tejada 1998).

3. Magnetic rings

Magnetic rings have long been theoretically investigated for calculating the thermodynamic properties of infinite chains (De Jongh & Miedema 1974). Recently, a large number of rings, comprising metal ions with quantum ($S = 1/2$) spins (Rentschler *et al.* 1996) or classical ($S = 5/2$) spins (Taft & Lippard 1990; Caneschi *et al.* 1996; Watton *et al.* 1998), and mixed quantum–classical spins, (alternating $S = 1/2$ and $S = 5/2$ spins) (Caneschi *et al.* 1988), has been reported. Also, the coupling in the rings can be varied at will, with examples of antiferromagnetic (Taft & Lippard 1990; Caneschi *et al.* 1988, 1996; Watton *et al.* 1998), ferromagnetic (Rentschler *et al.* 1996; Abbati *et al.* 1998; Blake *et al.* 1994) and ferrimagnetic (Caneschi *et al.* 1988) rings. The ground state of the rings varies from $S = 0$ for antiferromagnetic rings to $S = 12$ for some ferromagnetic or ferrimagnetic rings. Before moving on to describe the properties of the rings relevant to MQP, we will note, on passing, that so far essentially only rings with an even number of spins have been reported. This is unfortunate because it would be of extreme interest to have some example of antiferromagnetic rings with an odd number of unpaired spins, because, in this case, spin frustration effects might be observed (McCusker *et al.* 1991). These give rise to a highly degenerate ground state, which is unstable to many perturbations.

Rather surprisingly, the most interesting results so far have not come from the rings with a large ground spin state, namely the ferromagnetic or ferrimagnetic rings, but rather from the antiferromagnetic rings, which have an $S = 0$ ground state. In fact, these systems can be used as models for studying the macroscopic quantum coherence of the Néel vector, which tunnels between classical degenerate directions over many periods. This point was realized by Chiolero & Loss (1998), who calculated the quantum dynamics of the Néel vector by instanton methods. This semiclassical method, valid for large spins and in the continuum limit, allows the calculation of the tunnel splitting of the Néel vector modulated by an external magnetic field applied in a direction parallel to the ring. The presence of the external magnetic field tunes the tunnel barriers by introducing an effective anisotropy. If we pass from this semiclassical approach to the quantum approach appropriate for relatively small clusters, the presence of an external magnetic field in antiferromagnetic rings induces a change in the energies of the excited S states, as sketched in figure 3. The energy of the ground level is taken as zero, and the field is taken parallel to z. It is apparent

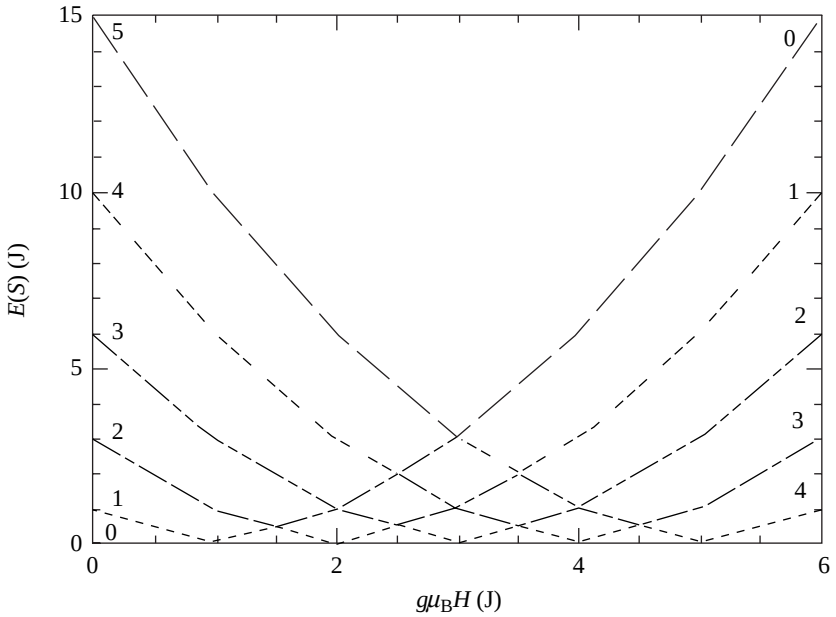

Figure 3. Field dependence of the energies of the low-lying S levels in antiferromagnetic rings. The energy of the ground level is taken as zero.

that at a given value of the field, the $S = 1$ state, which decreases its energy, crosses the $S = 0$ state, which is essentially field independent (Taft *et al.* 1994; Cornia *et al.* 1999*a*). When the two levels cross, the tunnel splitting is effectively quenched. However, the process is not limited to this crossover, because the level with $S = 2$ decreases its energy faster than that of $S = 1$, and eventually a second crossover occurs. In fact, the process continues on increasing field until the $S_{\max}$ level becomes the ground state. $S_{\max}$ is the spin state originated by putting all the individual spins parallel to each other. For a ring of N spins S_i, $S_{\max} = NS_i$. It is apparent that for such an antiferromagnetic ring there is the possibility of observing up to NS_i field-determined crossovers in the ground state.

The so-called ferric wheel (Taft & Lippard 1990), the structure of which is sketched in figure 1*a*, is the system that has been first investigated from this point of view. Pulsed magnetization measurements at 0.7 K provided the crossover up to $S = 9$ (Taft *et al.* 1994). The crossover energies can be quantitatively calculated for relatively small rings. However, a formula that gives the energies of the S states to a good approximation (Caneschi *et al.* 1996) is

$$E(S) = \frac{2J}{N} S(S+1), \tag{3.1}$$

where N is the number of spins in the ring. Equation (3.1) is most appropriate for rings in which the individual spins S_{I} are large. Therefore, it works well for quasi-classical spins, like $S = 5/2$, and is not useful for quantum spins like $S = 1/2$. From (3.1) we learn that the first crossover will occur when the Zeeman energy, $g\mu_{\mathrm{B}}H$ equals the energy of the lowest excited triplet, namely when $g\mu_{\mathrm{B}}H = 4NJ$. This is, in fact, the lower limit indicated by Chiolero & Loss (1998) for observing

tunnelling. It is also interesting that the following field values for tunnelling, or, in other words, the crossover fields, all appear at regular intervals, as expected on the basis of equation (3.1).

Stepped magnetization has been observed also in smaller iron(III) rings (Caneschi *et al.* 1996; Cornia *et al.* 1999*a*, *b*), like those depicted in figure 1*b*. In the centre of the ring, an alkali ion, Li^+ or Na^+, is present. In this case, it was also possible to investigate very small single crystals by new torque magnetometers using a sensitive cantilever to measure the magnetization. By measuring the magnetization in different crystal orientations, it was possible to directly measure the magnetic anisotropy of the excited S states. These investigations provided surprising results. In fact, it has been observed that the central alkali ion strongly influences both the isotropic exchange interaction, which passes from $14\,\mathrm{cm}^{-1}$ to $20\,\mathrm{cm}^{-1}$ for $\mathrm{M} = \mathrm{Li}^+$ and $\mathrm{M} = \mathrm{Na}^+$, respectively, and the magnetic anisotropy. In fact, the zero-field splitting of the first excited $S = 1$ level is $D = 1.16\,\mathrm{cm}^{-1}$ for the lithium and $D = 4.32\,\mathrm{cm}^{-1}$ for the sodium derivative.

All the measurements reported above are static measurements, which do not provide any information on the dynamics of the magnetization or on possible tunnelling phenomena. Dynamic measurements can, in principle, be made with a variety of techniques, ranging from AC susceptometry to magnetic resonance. In this respect, NMR is particularly appealing, because it can monitor the variations in the relaxation rate of the nuclear moments under the influence of the tunnelling of the electron magnetization. In fact, it can be expected that when two levels cross, the electron relaxation at low temperature is drastically influenced. Therefore, the field dependence of the nuclear relaxation rate should show anomalies corresponding to the crossover fields. Preliminary measurements performed on the ferric wheel in the temperature range 1.2–4.2 K show the presence of distinct maxima in the nuclear relaxation rates at the crossover fields (Julien *et al.* 1999). This may be experimental evidence of coherent tunnelling of the Néel vector in magnetic clusters.

4. Quantum effects in molecular ferrimagnets

The application of a strong external field may give rise to stepped variations in the magnetization also in ferrimagnets. Recently, a technique generating ultra-high magnetic fields up to 850 T by explosive compression of initial magnetic flux was implemented (Bykov *et al.* 1996). It was found that bulk ferrimagnets undergo a second-order (continuous) phase transition from the ferrimagnetic to a canted phase and then from the canted to ferromagnetic states (Zvezdin 1995). The same technique has recently been employed on the molecular cluster $[Mn_{12}O_{12}(CH_3COO)_{16}(H_2O)_4]$, Mn12Ac, the structure of which (Lis 1980) is sketched in figure 4, which has been investigated with a number of different techniques for its unique low-temperature magnetic behaviour, and for the first time some knowledge of the excited spin states has been achieved (Lubashevsky *et al.* 1999).

The ground state of Mn12Ac is now well established to be $S = 10$, as a result of non-compensation of the magnetic moments of eight manganese(III) ions, each with $S_i = 2$ and all parallel to each other, and four manganese(IV) ions, each with $S_j = 3/2$ and all antiparallel to the manganese(III) spins (Sessoli *et al.* 1993*b*). It is apparent that it is possible to increase the spin of the ground state by applying an external field that increases S. The available excited states with S larger than 10 are

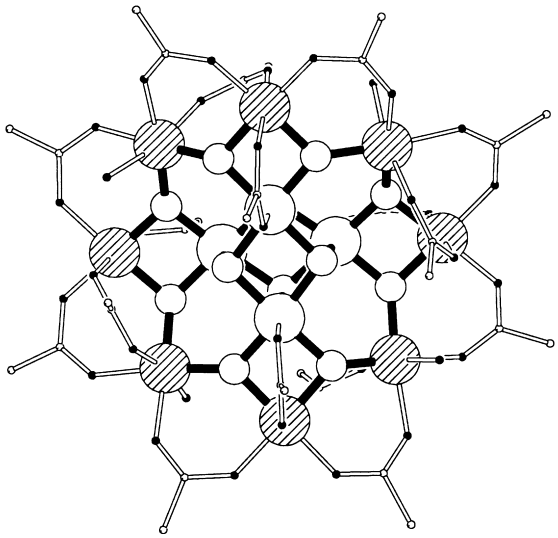

Figure 4. Sketch of the structure of Mn12Ac (after Lis (1980)).

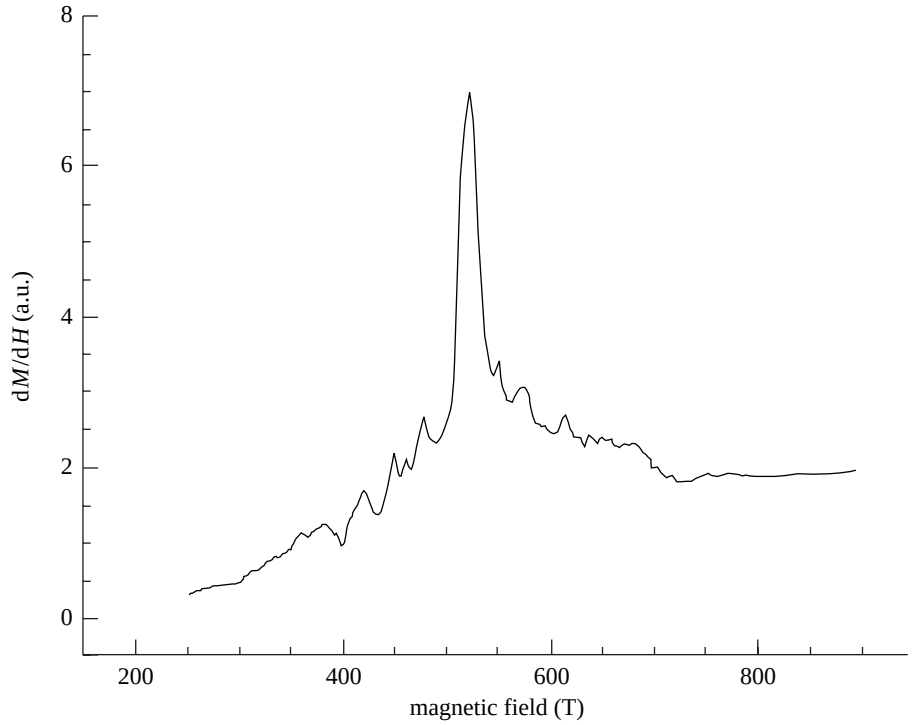

Figure 5. Differential magnetization of a single crystal of Mn12Ac in pulsed fields at 1.2 K. The duration of the pulses is of the order of 10^{-6} s.

Table 1. *Size of the matrices corresponding to the total spin states S of* Mn12Ac

S	$n(S)$	S	$n(S)$	S	$n(S)$
0	190 860	8	654 476	16	7656
1	548 370	9	428 450	17	2951
2	838 126	10	333 032	18	997
3	1 029 896	11	214 996	19	286
4	1 111 696	12	129 476	20	66
5	1 090 176	13	72 456	21	11
6	986 792	14	37 472	22	1
7	831 276	15	17 776		

$S = 11, 12, \ldots, 22$. The results of the pulsed experiments are shown in figure 5 as the $\mathrm{d}M/\mathrm{d}H$ versus H plot. No transition is observed up to $H = 350$ T, indicating that the lowest excited state with $S > 10$ is at least $350\,\mathrm{cm}^{-1}$ above the ground state. In fact, assuming a regular pattern of excited states, the crossover energies can be expressed as

$$H_{S\to S+1} = [E(S+1) - E(S)]/g\mu_{\mathrm{B}}. \tag{4.1}$$

Regular here means that the energies of the lowest $S+1$ and $S+2$ states in zero field obey the following conditions:

$$E(S+1) > E(S) \quad \text{and} \quad 2E(S+1) - E(S) < E(S+2). \tag{4.2}$$

Above 350 T, several spikes are observed, which strongly suggest that the energies of the excited states are quantized. Four spikes can be located at 382, 416, 448 and 475 T, suggesting that these are the crossover fields for $S = 11$, 12, 13 and 14, respectively. The following higher-intensity spike is presumably due to the fact that the crossover fields for more than one level occur at very similar values. In fact, we assign the spike to the crossover fields to $S = 15$, 16, 17 and 18. The higher-field spikes are assigned to the crossover fields to $S = 19$, 20, 21 and 22. No spikes are observed above 690 T, suggesting that the energy of the highest spin state is *ca.* $6000\,\mathrm{cm}^{-1}$ above the ground state. It would be desirable to attempt to record Raman spectra to confirm some of these values.

The calculation of the energies of the excited states of Mn12Ac is far from being trivial. In fact, the total number of spin states is 10^8, and even if the total spin symmetry is exploited in the best possible way, the size of the matrices corresponding to the different S values are as shown in table 1. In the Bible, the expression 'myriad of myriad' (corresponding to 10^8 in modern notation) means a number large beyond any limit.

It is apparent that the problem is tractable on the high-S side, where relatively small matrices must be calculated. Unfortunately, the crossover fields corresponding to these levels are less-well experimentally determined. We used a composite approach, using both a perturbation treatment and a direct calculation of the energies of the lowest-lying levels for each S value. In fact, the latter procedure could be used for $S = 16$–22, while the lower-lying levels were calculated through the perturbation approach. This, of course, underestimates the repulsion between levels with the same S. However, we found that although the absolute energies are not well

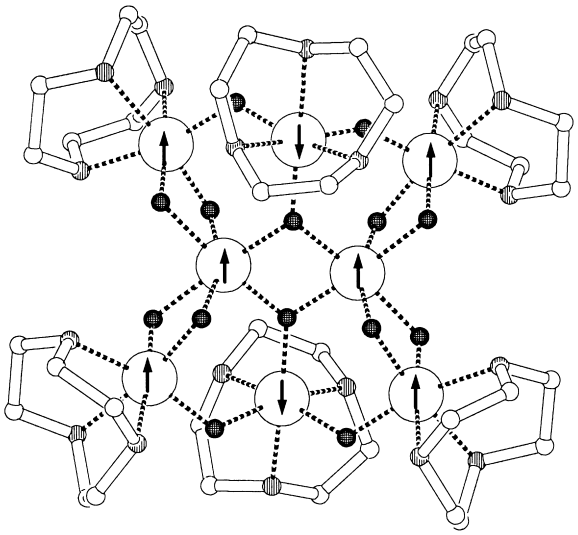

Figure 6. Sketch of the structure of Fe8 (after Wieghardt *et al.* (1984)).

calculated with this approach, the differences in crossover fields are reasonably well reproduced. The best-fit values of the parameters are: $J_1 = 122\ \mathrm{cm}^{-1}$, $J_2 = 60\ \mathrm{cm}^{-1}$, $J_3 = -11.2\ \mathrm{cm}^{-1}$ and $J_4 = 30\ \mathrm{cm}^{-1}$. These results are in qualitative agreement with the values of the coupling constants usually found in the analysis of the magnetic properties of smaller clusters containing manganese ions.

Molecular ferrimagnets are the systems that have, so far, provided the best examples for quantum tunnelling of the magnetization. The reason for this is easily understood: up to now, the ferrimagnets are the systems with the highest ground spin states and with the highest magnetic anisotropy. We do not see anything particularly special in ferrimagnets, except that, by chance, they have so far provided the best systems obeying the above requirements. The systems that I will treat to some extent are Mn12Ac, introduced above, and Fe8, the structure of which (Wieghardt *et al.* 1984) is sketched in figure 6. The spins depicted on the iron(III) ions provide a justification for the ground $S = 10$ state.

Both Mn12 and Fe8 have the $S = 10$ ground state, with the former having a uniaxial anisotropy (Sessoli *et al.* 1993*b*) and the latter having a biaxial anisotropy (Delfs *et al.* 1993; Barra *et al.* 1996). In both cases the low symmetry splitting of the ground states can be described (Barra *et al.* 1997) by the spin Hamiltonian:

$$H = D[S_z^2 - S(S+1)/3] + E(S_x^2 - S_y^2) + B_4^0 O_4^0 + B_4^4 O_4^4 + B_4^2 O_4^2. \tag{4.3}$$

The Hamiltonian assumes C_2 symmetry. The O_k^m are operator equivalents,

$$O_4^0 = 35S_z^4 - [30S(S+1) - 25]S_z^2 - 6S(S+1) + 3S^2(S+1)^2,$$
$$O_4^2 = \tfrac{1}{4}\{[7S_z^2 - S(S+1) - 5](S_+^2 + S_-^2) + (S_+^2 + S_-^2)[7S_z^2 - S(S+1) - 5]\},$$
$$O_4^4 = \tfrac{1}{2}(S_+^4 + S_-^4),$$

and the B_4^4 are parameters. Higher-order terms, in principle up to the 20th, are symmetry allowed, but they were not included for the sake of simplicity.

In Mn12Ac, the tetragonal symmetry of the cluster requires $E = 0$ and $B_4^2 = 0$. The values of the parameters, as obtained through EPR spectroscopy (Barra *et*

Table 2. *Low-symmetry parameters for* Mn12Ac *and* Fe8 (*all parameters in* K)

sample	D	E	B_4^0	B_4^4	B_4^2	ref.
Mn12Ac	-0.66	0	-3.17×10^{-5}	$+6\times10^{-5}$	—	Barra *et al.* 1997
Fe8	-0.2748	0.0464	—	—	—	Barra *et al.* 1996
Fe8	-0.2909	-0.0464	1.00×10^{-6}	8.54×10^{-6}	1×10^{-7}	Caciuffo *et al.* 1998

al. 1996, 1997) and inelastic neutron scattering (Caciuffo *et al.* 1998), are given in table 2.

The energies of the M states of the $S = 10$ multiplets for Mn12Ac and Fe8 are shown in figure 7. The levels are plotted according to the usual convention of the two separate potential wells, i.e the $+M$ states are plotted on one side and the $-M$ states are plotted on the other side. However, it must be stressed that this is reasonable to a good approximation for Mn12Ac, in which $E = 0$, while it is much less acceptable for Fe8. In fact, for the latter, M is no longer a good quantum number, and extensive mixing of the states occurs. Since the E term admixes states with M differing by ±2, its effect is large on the states with small M, while it has only a small effect on the states with large M. Therefore, for the latter, the approximation of the two potential wells is still acceptable. In fact, the pairs are quasi-degenerate up to $M = \pm5$, but the higher levels are heavily admixed. In particular, there are three reasonably well separated levels, and higher up there are two more quasi-degenerate pairs. Therefore, there is no $M = 0$ top level. In fact, the two highest quasi-degenerate levels are admixtures of various levels. One is the admixture of $M = 0$ with $M = \pm2$ and other even M values, while the other is the admixture of $M = \pm1$ with other odd M values. On the other hand, the levels are well behaved for Mn12. The largest splitting is observed between the $M = \pm2$ levels, due to the B_4^4 term, which mixes states differing by 4 in M.

It is quite remarkable that a very accurate description of the split levels of the ground $S = 10$ multiplet of Fe8 could be achieved through inelastic neutron-scattering experiments (Caciuffo *et al.* 1998). This technique does not, in general, produce good-quality spectra in systems having a large number of protons, and extensive deuteration is required. We performed our experiments on two grams of non-deuterated powder, and we obtained the detailed spectra shown in figure 8. The peaks correspond to transitions between M levels of the ground $S = 10$ state. These data allowed us to also determine the fourth-order crystal field parameters that had escaped the HF-EPR analysis.

At low temperature, both clusters show slow relaxation of the magnetization (Barra *et al.* 1996; Sessoli *et al.* 1993*a*) with lower blocking temperature for Fe8. This is in qualitative agreement with the fact that at low temperature the pairs of levels with large M are populated. The magnetization can revert its sign if the spin value passes from $M = -S$ to $M = -S + 1$, then to $M = -S + 2$, and so on up to the top of the barrier, or to a level from which it can shortcut to the opposite side of the barrier. It is customary to take $\Delta = |D|S^2$ as a rough estimation of the height of the barrier. In this sense, it is apparent that the barrier for Mn12Ac is higher than for Fe8. Furthermore, the latter has more opportunities to shortcut given the large admixture of the levels with small M. The magnetization of Mn12Ac has been found to follow the Arrhenius law with $\tau_0 = 2\times10^{-7}$ s, and $\Delta/k = 62$ K, in rea-

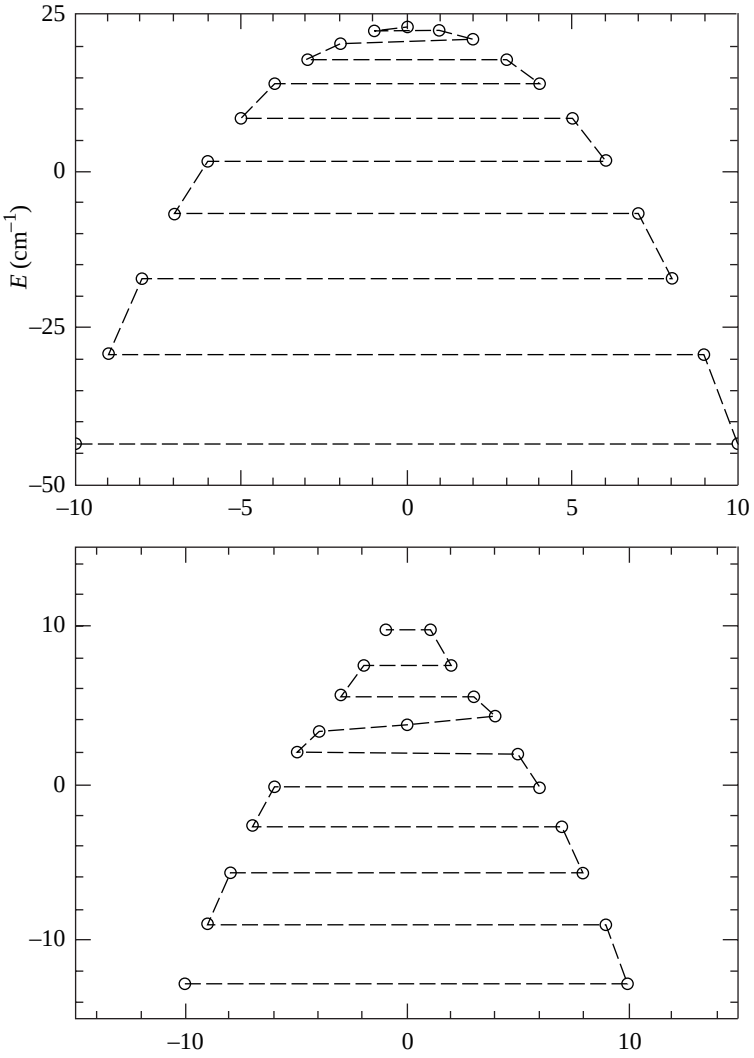

Figure 7. Energies of the M components of the $S = 10$ ground states of Mn12Ac (top), and Fe8 (bottom). The lowest components are $M = \pm 10$, while the highest components are heavily admixed for Fe8 (see text).

sonable agreement with the value that can be calculated from the zero-field splitting parameter. Fe8 does not quite obey the Arrhenius law, except in small temperature ranges.

Both clusters show evidence of thermally assisted quantum tunnelling (Thomas *et al.* 1996; Friedman *et al.* 1997; Sangregorio *et al.* 1997). The meaning of this expression is that when a spin is in the M state, with $M < S$, it has a finite probability of tunnelling to the $-M + n$ state when the two levels have the same energy (Luis *et al.* 1998). n is an integer that depends on the value of the magnetic field applied parallel to the easy axis of the magnetization of the clusters needed in order to put the two levels at the same energy. For the simple case of axial symmetry,

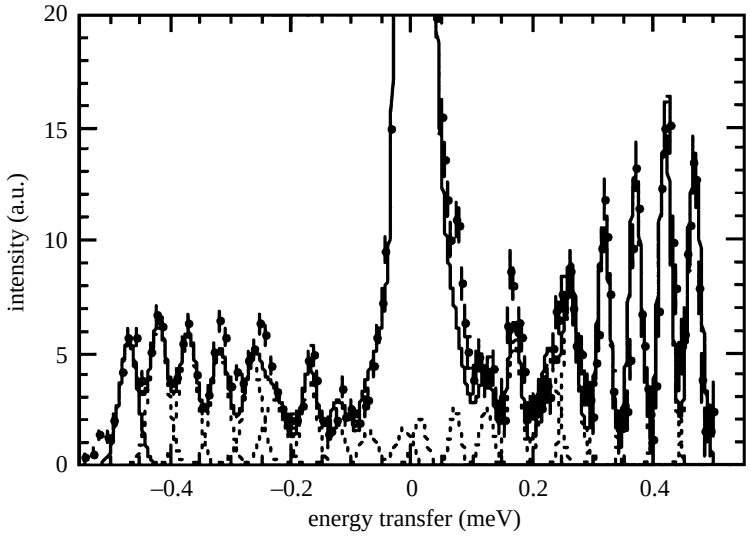

Figure 8. Inelastic neutron scattering of Fe8 at 10 K.

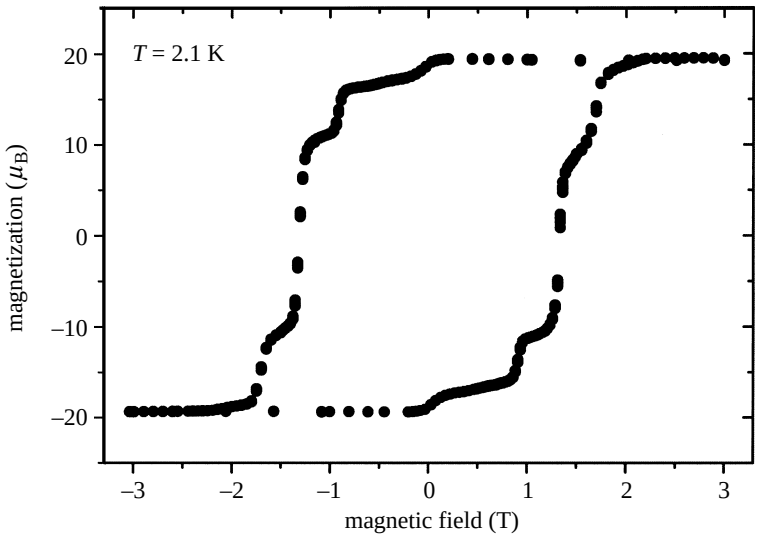

Figure 9. Stepped hysteresis of a single crystal of Mn12Ac at 2.1 K. The field is parallel to the tetragonal axis of the cluster.

including only second-order terms

$$H_n = nD/(g\mu_B). \tag{4.4}$$

The efficiency of this mechanism has been best observed in a single crystal of Mn12Ac, whose temperature-dependent hysteresis (Thomas *et al.* 1996) is shown in figure 9. The sharp steps correspond to fast relaxation, determined by quantum tunnelling between degenerate pairs of levels. At different values of the field the levels are not at the same energy, the quantum tunnelling is therefore quenched. Similar results were observed (Sangregorio *et al.* 1997) for Fe8, and the field corresponding

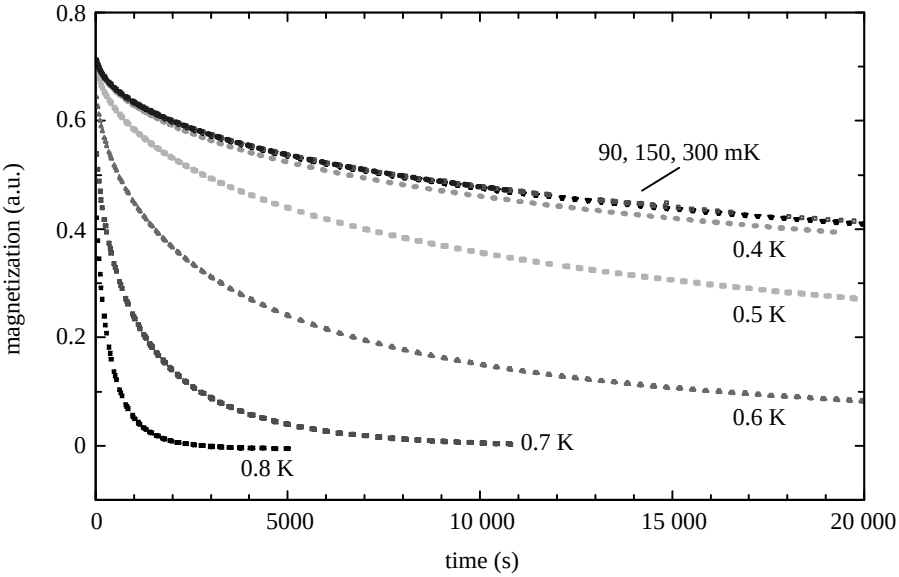

Figure 10. Time dependence of the decay of the magnetization of Fe8 below 1 K. Below 300 mK the relaxation becomes independent of temperature.

to the strong tunnelling effects can be calculated with high accuracy, adding the Zeeman term to the spin Hamiltonian (4.1).

At very low temperature, below 2 K for Mn12Ac, the $M = \pm S$ levels are the only populated ones, but no clear evidence of tunnelling has been achieved. In fact, the transverse anisotropy is so small that the tunnelling frequency between these two levels is vanishingly small. It must be mentioned that the Arrhenius law suggests that at 1 K the relaxation time of the magnetization becomes of the order of billions of years. There is no doubt that under these conditions the Mn12Ac clusters behave as tiny magnets. It is also interesting to notice that, although the size of the clusters is so small that they are clearly within the quantum limit, quantum tunnelling is completely inefficient at low temperature.

Matters are different with Fe8, where the transverse magnetic anisotropy is large enough to establish the quantum tunnelling regime at low temperature. This is clearly shown by figure 10, where the decay of the magnetization of Fe8 becomes (Sangregorio *et al.* 1997) clearly temperature independent below 300 mK.

Recently, another unique quantum feature has been observed (Wernsdorfer & Sessoli 1999) in Fe8, which represents the first experimental evidence of the so-called Berry phase in magnets (Berry 1984). A semiclassical approach of the instanton type suggests that if a field is applied parallel to the hard axis, x, of a magnetic particle characterized by a giant spin S, the tunnelling splitting oscillates regularly as a function of the applied field (Garg 1993). The tunnel splitting is quenched whenever the following condition is met:

$$H_m = (S - m + 1/2)\Delta H, \tag{4.5}$$

where m is an integer ranging from 1 to S. If only the second-order terms of the spin

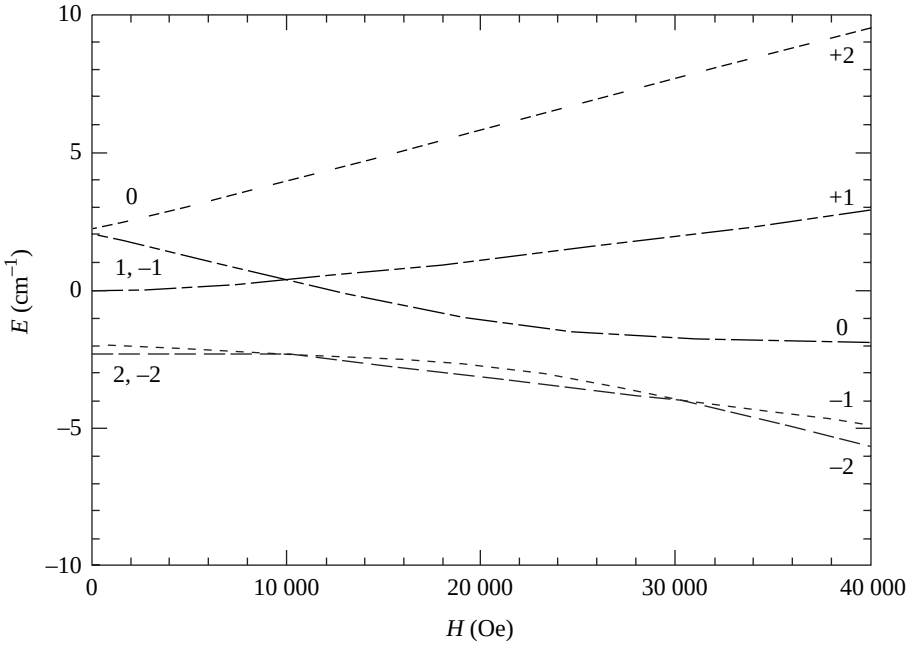

Figure 11. Field dependence of the M energy levels of an S multiplet. The field is applied parallel to the hard axis. The different labelling of the levels on the right and on the left corresponds to weak and strong field limits, respectively.

Hamiltonian (3.1) are included,

$$\Delta = [2E(E-D)]^{1/2}2/(g\mu_{\mathrm{B}}). \tag{4.6}$$

Since the tunnel splitting is responsible for the tunnelling relaxation it must be expected that a direct measurement of the relaxation rates should show maxima at the fields H_m given by equations (4.5) and (4.6).

Before proceeding further on this point, we want to stress that for particles with relatively small spins the conditions described by equations (4.5) and (4.6) find a simple interpretation. The results of calculation applied to an $S = 2$ state with $D = -1\ \mathrm{cm}^{-1}$, $E/D = 1/3$ in the presence of a variable field parallel to x are shown in figure 11. The levels are all non-degenerate in zero field, and in the presence of the field they vary their energies and the admixtures. The lowest-lying levels, which in axial symmetry would be $M = \pm 2$, initially decrease their separation, then they become degenerate at $H = 1.01$ T. At the same field, the upper levels, which in axial symmetry would be $M = \pm 1$, also cross. A further increase of the field determines a second crossing of the lowest lying levels at $H = 3.03$ T. If the calculations are repeated, for instance for $S = 3$, the crossing fields will remain the same, except that there would be an additional one for the lowest-lying levels at 5.05 T. Again, what is extremely interesting is to see that the semiclassical and the quantum exact calculations give the same results.

If analogous calculations are performed for half-integer spins, the splitting is calculated as zero in zero field as expected for Kramers doublets. The transverse field removes the degeneracy and the pairs of levels to cross each other with the periodicity calculated through equations (4.5) and (4.6).

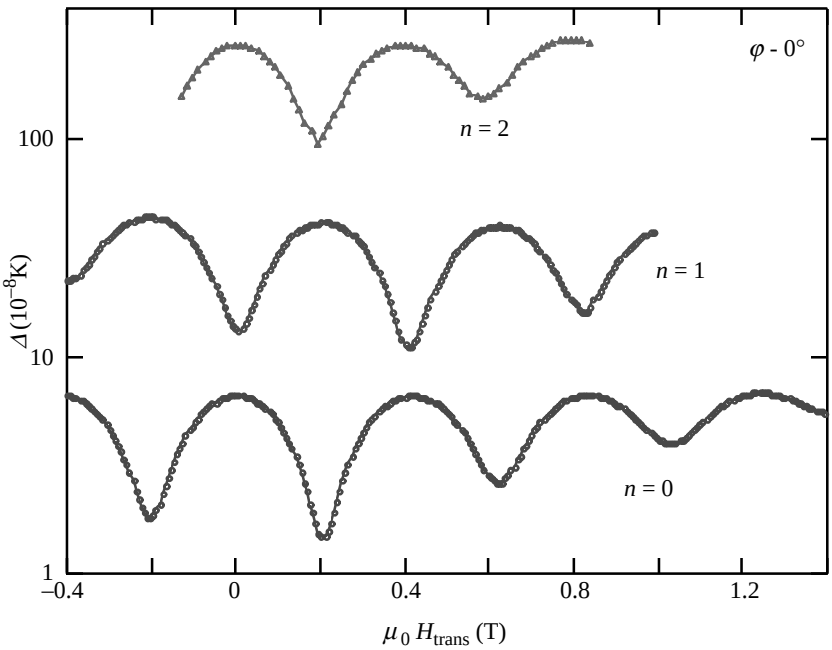

Figure 12. Experimental tunnel splitting of the lowest $M = \pm 10$ components of Fe8. The transverse field is applied parallel to the hard axis. An AC field is applied parallel to the easy axis. The n values correspond to the resonances defined in equation (4.4).

The exciting result is that for the first time Wernsdorfer & Sessoli (1999) have directly measured the splitting of the levels by measuring the tunnelling rate of Fe8 clusters in the presence of two applied fields. They used an array of microSQUIDs to measure the relaxation of the magnetization in the presence of an AC field that sweeps over the entire resonance transition, which is determined by dipolar and hyperfine fields. The AC field is applied parallel to the easy axis, while the static field is applied parallel to the hard axis. The results are shown in figure 12 for $H_z = 0$ and for H_z corresponding to the first resonance described by equation (4.5). There are two things to be noticed. The first is the periodicity of the maxima in the relaxation rate, which correspond to the fields at which the lowest levels have the maximum tunnel splitting. The second is that there is a strong parity effect. In fact, for n even, the maxima in the tunnelling rates correspond to the H_m fields of equations (4.5) and (4.6). The parity effect has a symmetry origin analogous to the Kramers degeneracy of the spin states with half-integer S. These measurements were able, for the first time, to determine very small energy splittings of the order of 10^{-8} K, which are not accessible by spectroscopic techniques.

In the semiclassical picture, the observed oscillations are due to topological quantum interference of two tunnel paths of opposite directions. The tunnelling transitions of the magnetization vector between two minima in a biaxial system can be schematized as given by two symmetrical paths in the plane perpendicular to the hard axis. In zero field, the two quantum spin paths give constructive interference when S is an integer, while a quench of the tunnelling splitting is given by destructive interference for half-integer spins (Bogacheck & Krive 1992; Loss *et*

al. 1992; Golyshev & Popkov 1995). When the field is applied along the hard axis, a destructive–constructive interference of the quantum spin phase (known as the Berry phase (Berry 1984)), is observed and gives rise to oscillations in the tunnelling rate, similar to the Aharonov–Bohm oscillations of the conductivity in mesoscopic rings (Imry 1977).

These experiments on Fe8 have, for the first time, evidenced this phenomenon in magnetic systems and have again shown the great impact of molecular clusters for the study of magnetism at the mesoscopic scale. The Berry phase and the Haldane gap and the related parity effects in magnetic materials have been debated for a long time, but experiments on traditional nanosized particles have failed to reveal them. The Fe8 systems are the ideal candidates because of their biaxial anisotropy, their pure observable tunnelling regime at accessible temperatures, and their intrinsic quantum nature.

5. Conclusions

Molecular clusters are providing exciting new perspectives at the frontier between the quantum and the classical world. I believe that in this article I have shown how different quantum effects can be observed through the collaboration between physicists and chemists who have become able to speak to each other. I also feel that these materials are extremely productive, not only for the development of new basic science but also for new applications. If quantum effects are important for developing quantum computers, molecular clusters of increasing size and complexity provide an almost infinite number of new possibilities.

The results of the Florence laboratory have been obtained through collaboration with many groups throughout the world. They are all duly acknowledged by the references. They have been obtained thanks to the enthusiasm of my collaborators in Florence and Modena: Andrea Caneschi, Andrea Cornia, Claudio Sangregorio, Alessandro Lascialfari. The highest credit, however, should be given to Roberta Sessoli, who was the actual initiator of the field. The financial support of MURST, CNR and PFMSTAII is gratefully acknowledged.

References

Abbati, G. L., Cornia, A., Fabretti, A. C., Caneschi, A. & Gatteschi, D. 1998 *Inorg. Chem.* **37**, 1430.

Awschalom, D. D., DiVincenzo, D. P., Grinstein, G. & Loss, D. 1993 *Phys. Rev. Lett.* **71**, 4276.

Barra, A. L., Debrunner, P., Gatteschi, D., Schulz, C. & Sessoli, R. 1996 *Europhys. Lett.* **35**, 133.

Barra, A. L., Gatteschi, D. & Sessoli, R. 1997 *Phys. Rev.* B **56**, 8192.

Bastard, G. & Brum, J. A. 1986 *IEEE J. Quantum Electron.* **22**, 1625.

Berry, M. V. 1984 *Proc. R. Soc. Lond.* A **392**, 45.

Blake, A. J., Grant, C. M., Parsons, S., Rawson, J. M. & Winpenny, R. E. P. 1994 *J. Chem. Soc. Chem. Commun.*, p. 2363.

Bogachek, E. N. & Krive, I. V. 1992 *Phys. Rev.* B **46**, 14 559.

Bykov, A. I., Dolotenko, M. I., Kolokol'chikov, N. P., Pavlovskii, A. I. & Tatsenko, O. M. 1996 *Physica* B **216**, 215.

Caciuffo, R., Amoretti, G., Murani, A., Sessoli, R., Caneschi, A. & Gatteschi, D. 1998 *Phys. Rev. Lett.* **81**, 4794.

Caldeira, A. O. & Leggett, A. J. 1981 *Phys. Rev. Lett.* **46**, 211.

Caneschi, A., Gatteschi, D., Laugier, J., Rey, P., Sessoli, R. & Zanchini, C. 1988 *J. Am. Chem. Soc.* **110**, 2795.

Caneschi, A., Cornia, A., Fabretti, A. C., Foner, S., Gatteschi, D., Grandi, R. & Schenetti, L. 1996 *Chem. Eur. J.* **2**, 2329.

Chiolero, A. & Loss, D. 1998 *Phys. Rev. Lett.* **80**, 169.

Chudnovsky, E. M. & Tejada, J. 1998 *Macroscopic quantum tunnelling of the magnetic moments*. Cambridge University Press.

Cornia, A., Jansen, G. M. & Affronte, M. 1999*a* *Phys. Rev.* B. (In the press.)

Cornia, A., Affronte, M., Jansen, A. G. M., Abbati, G. L. & Gatteschi, D. 1999*b* *Angew. Chem. Int. Ed. Engl.* **38**, 2264.

De Jongh, L. J. & Miedema, A. R. 1974 *Adv. Phys.* **23**, 1.

Delfs, C., Gatteschi, D., Pardi, L., Sessoli, R. & Hanke, D. 1993 *Inorg. Chem.* **32**, 3099.

Deutsch, D. & Jozsa, R. 1985 *Proc. R. Soc. Lond.* A **239**, 553.

Friedman, J. R., Sarachik, M. P., Tejada, J. & Ziolo, R. 1997 *Phys. Rev. Lett.* **76**, 3830.

Garg, A. 1993 *Europhys. Lett.* **22**, 205.

Garg, A. 1995 *Science* **272**, 424.

Gatteschi, D., Caneschi, A., Pardi, L. & Sessoli, R. 1994 *Science* **265**, 1054.

Gider, S., Awschalom, D. D., Douglas, T., Mann, S. & Chaparala, M. 1995 *Science* **268**, 77.

Gider, S., Awschalom, D. D., DiVincenzo, D. P. & Loss, D. 1997 *Science* **272**, 425.

Golyshev, V. Yu & Popkov, A. F. 1995 *Europhys. Lett.* **29**, 327.

Gunther, L. & Barbara, B. (eds) 1995 *Quantum tunneling of magnetization—QTM 94*. Wiley.

Halperin, B. I., Lee, P. A. & Read, N. 1993 *Phys. Rev.* B **47**, 7312.

Imry, Y. 1977 *Introduction to mesoscopic physics*. Oxford University Press.

Jain, J. K. 1989 *Phys. Rev. Lett.* **63**, 199.

Julien, M. H., Jang, Z. H., Lascialfari, A., Borsa, F., Horvatic, M., Caneschi, A. & Gatteschi, D. 1999 *Phys. Rev. Lett.* **83**, 227.

Langer, J. J. 1967 *Ann. Phys.* **41**, 108.

Lis, T. 1980 *Acta Cryst.* B **36**, 2042.

Loss, D., DiVincenzo, D. P. & Grinstein, G. 1992 *Phys. Rev. Lett.* **69**, 3232.

Lubashevsky, I. A. (and 12 others) 1999 (Submitted.)

Luis, F., Bartolome, J. & Fernandez, J. F. 1998 *Phys. Rev.* B **57**, 1.

McCusker, J. K., Schmitt, E. A. & Hendrickson, D. N. 1991 In *Magnetic molecular materials* (ed. D. Gatteschi, O. Kahn, J. Miller & F. Palacio). NATO-ASI Series, vol. E198. Kluwer.

Morrish, R. 1966 *The physical principles of magnetism*. Wiley.

Prokof'ev, N. V. & Stamp, P. C. E. 1996 *J. Low Temp. Phys.* **104**, 143.

Rentschler, E., Gatteschi, D., Cornia, A., Fabretti, A. C., Barra, A.-L., Shchegolikhina, O. I. & Zhdanov, A. A. 1996 *Inorg. Chem.* **35**, 4427.

Sangregorio, C., Ohm, T., Paulsen, C., Sessoli, R. & Gatteschi, D. 1997 *Phys. Rev. Lett.* **78**, 4645.

Sessoli, R., Gatteschi, D., Caneschi, A. & Novak, M. 1993*a* *Nature* **356**, 141.

Sessoli, R., Tsai, H. L., Schake, A. R., Wang, S., Vincent, J. B., Folting, K., Gatteschi, D., Christou, G. & Hendrickson, D. N. 1993*b* *J. Am. Chem. Soc.* **115**, 1804.

Stamp, P. C. E. 1996 *Nature* **383**, 125.

Taft, K. L. & Lippard, S. J. 1990 *J. Am. Chem. Soc.* **112**, 9629.

Taft, K. L., Delfs, C. D., Papaefthymiou, G. C., Foner, S., Gatteschi, D. & Lippard, S. J. 1994 *J. Am. Chem. Soc.* **116**, 823.

Tejada, J. 1995 *Science* **272**, 425.

Thomas, L., Lionti, F., Ballou, R., Gatteschi, D., Sessoli, R. & Barbara, B. 1996 *Nature* **383**, 145.

Watton, S. P., Fuhrmann, P., Pence, L. E., Caneschi, A., Cornia, A., Abbatti, G. L. & Lippard, S. J. (eds) 1997 *Angew. Chem. Int. Ed. Engl.* **36**, 2774.

Wernsdorfer, W. & Sessoli, R. 1999 *Science* **284**, 133.

Wieghardt, K., Pohl, K., Jibril, I. & Huttner, G. 1984 *Angew. Chem. Int.* **23**, 77.

Zvezdin, A. K. 1995 In *Handbook of magnetic materials* (ed. K. H. J. Buschow), vol. 9, p. 405. Elsevier.